Abstract

This report documents and details the design and analysis of an impeller for a centrifugal fan. The objective of this design project was to design an impeller that would produce a desired performance curve at a given rotational speed. After calculating initial guess blade angles, variations in the angles and shapes were simulated using PumpLinx®, and the final design was 3D printed and tested. The results were compared to the predicted performance curve and the efficiency curve was plotted.

The initial step in designing the impeller to meet the design criteria was to determine initial guesses for the blade angles. Using the design parameters that could not be changed, including the number of blades, blade thickness and impeller diameters, and geometric relations of the direction of entering and exiting air, the blade angles were determined. Design variations were tested using SimericsMP+ PumpLinx® to analyze the results of the design. After iteratively changing the impeller design until criteria was met, the design was 3-D printed. The final design was then tested in a testing apparatus provided by the UF lab.

The final impeller was tested at 1500 rpm and 2500 rpm, while the design criteria only specified a performance curve for 2500 rpm. The results given by the test fell within an average of 16.5% off from the desired curve, with points as high as 41.6% off and as low as 2.0% off. The maximum head was found to be 36.5 m, and the peak efficiency was found to be 25.1% at 0.08 kg/s, which was the specified design flowrate.

Introduction

The objective of this report was to design an impeller that produced a desired performance curve and to present the results and analysis resulting from testing the design both virtually and physically. The new impeller design was first tested using Computation Fluid Dynamic testing, and then built using a 3-D printer and tested using the centrifugal fan apparatus in the lab. The performance curves and efficiency curves were compared and reported in this paper.

The design process for designing the impeller was as follows. A Solidworks impeller template file was provided containing all of the dimensions required to fit the impeller in the testing apparatus. Dimensions given included the outer diameter, D_2, the inner diameter, D_1, the thickness of the blades, t, the blade height at the outer rim of the impeller, b_1, and the blade height at the inner diameter or the impeller, b_2. These parameters did not change. Also provided in the design criteria was the shut off head, h_o, design flow rate, Q_o, design rpm, ω_o, the ‘a’ coefficient of the performance curve, the ‘b’ coefficient of the performance curve, and the number of blades, n.

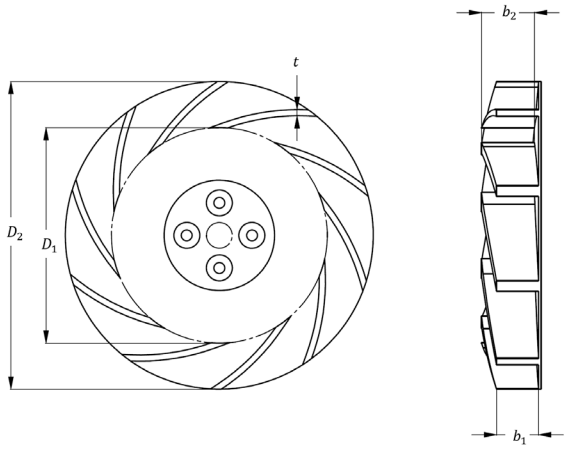

Figure 1: The impeller template with provided dimensions. These dimensions were left constant to ensure the impeller fit withing the testing apparatus.

The parameters we were responsible for finding and changing in the impeller design included the blade entrance angle, β_1, the blade exit angle, β_2, and the shape of the blade. The entrance and exit angles of the blade are defined from the tangent to the circle which the respective end of the blade lies on.

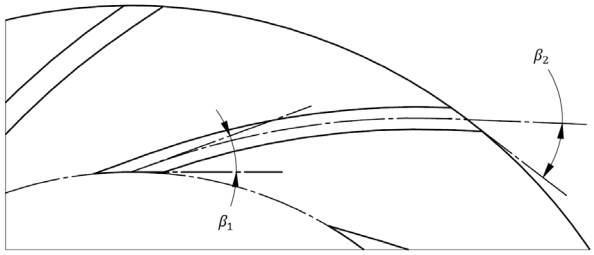

Figure 2: A drawing of the impeller blades with the entrance and exit angles labeled.

Using the specified parameters our group determined the appropriate blade angles that would theoretically allow for our design to satisfy the given parameters. The blade angle was adjusted in Solidworks and was tested using computation fluid dynamic testing in PumpLinx®. Using the resulting pressures and air velocities, we analyzed the data to find the head and flowrate in order to produce a performance curve.

The equation to determine the blade angles was derived using the Euler-Turbomachine equation in combination with the desired performance curve and geometry of the impeller blades. The derivation was as follows:

The ideal head loss in a centrifugal pump can be found from using the law of conservation of momentum and relates the velocities of the impeller blade and fluid entering the impeller to the head loss. The equation is as follows:

$$h = \frac{U_2 \cdot V_2 - U_1 V_1}{g}$$

Where U is the velocities of the impeller blade (ω·r) and V are the tangential and normal velocities of the fluid. This equation can be reduced due to the assumption that there is no fluid velocity in the direction of the blade rotation (V_1=0) and can be written to be in terms of the angular velocity, radius, and tangential velocities of the fluid.

V_t represents the tangent velocity, and x represents the exit velocity of the air. When looking at β_2, the assumption will be made that $V_{t1} = 0$.

$$h = \frac{\omega_o}{g}(r_2 V_{t2} - r_1 V_{t1}) = \frac{\omega_o r_2 V_{t2}}{g}$$

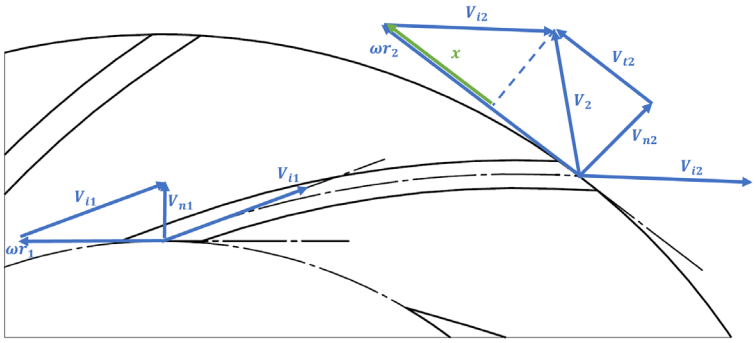

Figure 3: A visual representation of the direction of air flow as it enters and exits the blades.

Using trigonometry and the direction of air flow exiting the impeller, we get the following relationships which can be simplified and substituted into the head equation.

$$\tan\beta_2 = \frac{V_{n,2}}{x}$$

$$x = \frac{V_{n,2}}{\tan\beta_2} = \frac{Q_O/A_2}{\tan\beta_2}$$

$$V_{t,2} = \omega_o r_2 - x = \omega_o r_2 - \frac{Q_o/A_2}{\tan\beta_2}$$

The area in the equation is the area of the space between outer edges of the blades, which can be found by

$$A_2 = \pi \cdot D_2 \cdot b_2 - n \cdot b_2 \cdot t' = b_2(\pi D_2 - nt')$$

Substituting these equations into the head equation, it becomes

$$h = \frac{\omega_o r_2}{g}\left(\omega_o r_2 - \frac{\frac{Q_o}{A_2}}{\tan\beta_2}\right) = \frac{\omega_O^2 r_2^2}{g} - \frac{\omega_O r_2\left(\frac{Q_O}{b_2}\right)(\pi D_2 - nt')}{\tan\beta_2}$$

Taking the derivative of the equation with respect to the flowrate results in

$$\frac{dh}{dQ} = \frac{\omega_O r_2}{g b_2\left(\pi D_2 - n\frac{t}{\sin\beta_2}\right)\tan\beta_2}$$

The same trigonometric relationships apply when finding the angle β_1, resulting in the following equations.

$$V_{n,2} = V_1$$

$$\tan\beta_1 = \frac{\frac{Q_O}{A_1}}{r\omega_O}$$

$$t' = \frac{t}{\sin\beta_1}$$

$$A_1 = \pi D_1 b_1 - n b_1 t' = \pi D_1 b_1 - n b_1 \frac{t}{\sin\beta_1}$$

β_1 can now be found by substituting the value of A_1 into the trigonometric function of the velocity diagram at the inlet which results in the following equation:

$$\tan(\beta_1) = \frac{Q_O}{r\omega_O\left(\pi b_1 D_1 - n b_1 \frac{t}{\sin\beta_1}\right)}$$

Given blade thickness, performance curve slope, the number of blades, design flowrate, rpm, and a shutoff head, the β_1 and β_2 angles were calculated using a simultaneous solution approach where the intersection of the left-hand side and the right-hand side of the equations are the respective β angles.

The testing of the impeller occurred after the β angles were defined and were done using PumpLinx® for the CFD analysis. The impeller was tested to determine the head and efficiency curves at the design rpm of 2500. 200 iterations were set to allow the simulation to come to steady state. We recorded pressures and velocities at the inlet, and before and after the impeller with exit nozzle sizes of 100%, 70%, 50%, 40%, 30%, 25%, 20%, 15%, 10%, and 5%. The performance and efficiency curves were produced from our analysis by calculating the head and flowrate assuming that the difference in elevation and velocity heads are negligible. The resulting performance curve was then compared to the desired performance curve and the percent error was recorded. We then altered the impeller by slightly changing the β angles and the shape of the blades while preserving the blade's original thickness, until we achieved an average error below 5%.

The final impeller design was 3-D printed and installed into a centrifugal fan to determine the actual head and performance curves of our design. The impeller was tested at 1500 RPM and 2500 RPM with nozzles 100%, 90%, 70%, 50%, 40%, 30%, 25%, 20%, 15%, 10%, 5%, and 0%. The resulting performance and efficiency curves were compared to the simulated and the given curves and the error between them was studied. The aim for the designed impeller was for it to produce a performance curve that was within 15% error of the given performance curve and for the efficiency curve to be similar to the simulated efficiency curve. The reason for raising the error to 15% is that there were many imperfections with the centrifugal testing apparatus that could've caused discrepancies between the values such as air leaks.

Modeling Approach

The parts of the impeller we were responsible for designing included the blade entrance and exit angles, as well as the shape of the blade. The first step in the design approach was to determine initial guesses for the blade angles. By using the geometry of the blade angles and the direction of entering or exiting air in combination with the Euler Turbomachine equation and desired performance curve, we derived the equations as shown in the introduction. Using these equations, we found blade angles for an initial design. We determined the entrance blade angle, β_1, to be 15.01° and the exit blade angle, β_2, to be 36.67°.

The next steps were to model and test the initial angles that were found virtually. To model the impeller, a template was provided with the necessary geometry and dimensions to ensure that the impeller fit withing the testing rig. To generate the blades the first time, we used a blade shape of a single, constant arc with endpoints on the inner and outer diameter and defined only by the entrance and exit angles. The arc was sketched and defined as the centerline, and the sketch was then offset by 3/32" on each side of the arc in order to make a blade that was a consistent 3/16" thick. The ends of the blade were closed off by the inner and outer diameter of the impeller, with no rounding of the edges.

The model was then input into a PumpLinx® file containing the rest of the testing apparatus. The testing parameters and part features were input into the model, including rpm testing fluid, and wall roughness. The impeller was tested at 2500 RPM with 200 iterations to allow for the readings to come to steady state. The pressure and velocity were recorded at the entrance of the inlet, just before the impeller, and just after the impeller. The head was then calculated from the pressure readings and plotted against the volumetric flowrate.

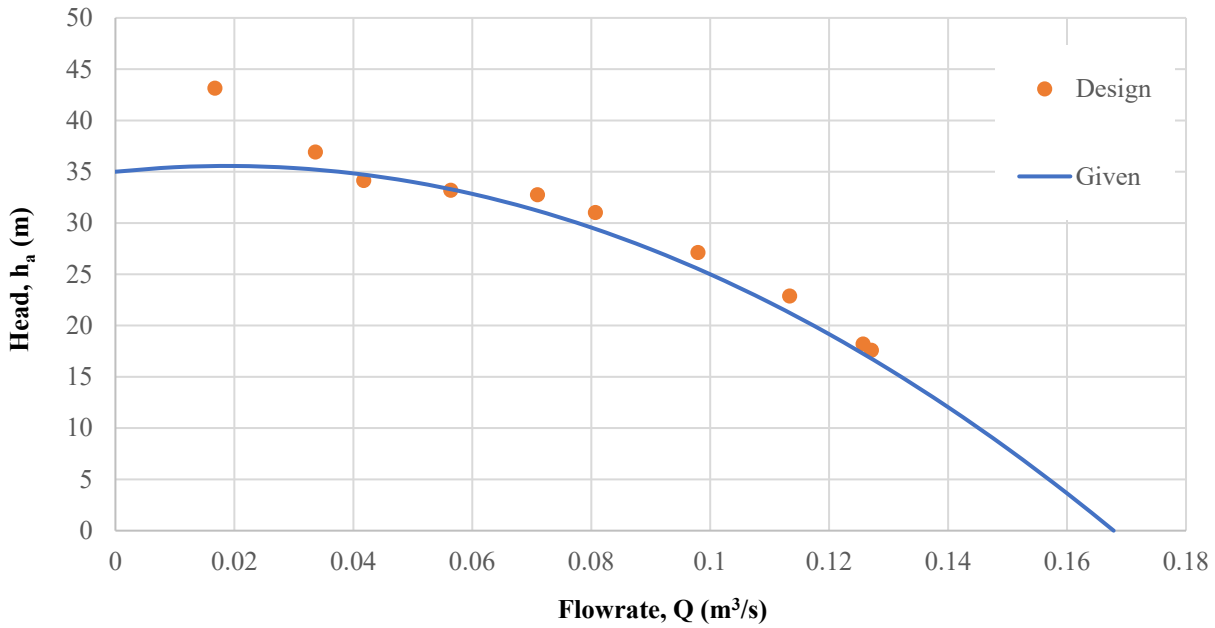

Figure 4: The first version of the designed impeller's head is plotted vs. flowrate using the calculated β angles and not altering the blade shape.

After testing the initial design, we tried varying different aspects of the blades to determine how the factors affected the performance curve. We changed both blade angles and the blade shape individually, such that we could determine what affect each change made and find the right combinations of angles and blade shape. We started by increasing and decreasing β_1, and then increasing and decreasing β_2. After picking the blade angles that gave us the best results, we adjusted the shape of the blade. This primarily consisted of how much of the blade would be curved versus linear, and where the linear portion was located. This process is described in further detail later in the report.

We found the combination of a β_1 of 15.01°, a β_2 of 35°, and a blade shape with a linear entrance and exit gave us a performance curve that almost matched the desired curve. The average error of this curve was around 4% off. This final design was then sent to be 3D printed for physical testing. The physical impeller was then tested using a testing apparatus in the lab at 1500 RPM and 2500 RPM. The differential manometer fluid heights were recorded in the same locations as the PumpLinx®. The head and flowrate values were calculated and plotted. The testing procedure and results are discussed in further detail later in the report.

Sample Calculations

Entrance Blade Angle: In the following equation β_1 is the entrance angle of the blade relative to the normal of the impeller, Q_O is the design flowrate, r_1 is the inner radius of the impeller, ω_O is the design angular velocity of the impeller, b_1 is the inner impeller height, n is the number of blades, D_1 is the inner diameter of the impeller, and t is the thickness of the blade.

$$\tan(\beta_1) = \frac{Q_O}{r_1 \cdot \omega_O \cdot \left(\pi \cdot b_1 \cdot D_1 - n \cdot b_1 \cdot \frac{t}{\sin(\beta_1)}\right)}$$

$$\tan(\beta_1) = \frac{0.08\ \frac{m^3}{s}}{(0.083\ m) \cdot \left(2500 \frac{rev}{min} \cdot \frac{min}{60\text{s}} \cdot \frac{2\pi\ rad}{rpm}\right) \cdot \left(\pi \cdot (0.04065\ m) \cdot (0.166\ m) - 10 \cdot (0.04065\ m) \cdot \frac{(0.0047625\ m)}{\sin(\beta_1)}\right)}$$

$$\tan(\beta_1) = \frac{0.08\ \frac{m^3}{s}}{\left(21.73 \frac{m \cdot rad}{s}\right) \cdot \left((0.02120\ m^2) - \frac{0.00194\ m^2)}{\sin(\beta_1)}\right)}$$

$$\tan(\beta_1) = \frac{0.08\ \frac{m^3}{s}}{\left(0.4907 \frac{m^3 \cdot rad}{s}\right) - \left(\frac{0.04207 \frac{m^3 \cdot rad}{s}}{\sin(\beta_1)}\right)}$$

$$0.08\ \frac{m^3}{s} = \tan(\beta_1)\left[\left(0.4907 \frac{m^3 \cdot rad}{s}\right) - \left(\frac{0.04207 \frac{m^3 \cdot rad}{s}}{\sin(\beta_1)}\right)\right]$$

$$\beta_1 = 0.2620\ rad \cdot \frac{180°}{\pi\ rad} = 15.01°$$

Exit Blade Angle: In the following equation β_2 is the exit angle of the blade relative to the normal of the impeller, $\frac{dH}{dQ}$ is the slope of the performance curve at the desired flowrate (Q = 0.08 $\frac{m^3}{s}$), g is the gravitational constant, r_2 is the outer radius of the impeller, ω is the desired angular velocity of the impeller, b_2 is the outer impeller height, n is the number of blades, D_2 is the outer diameter of the impeller, and t is the thickness of the blade.

$$\frac{dH}{dQ} = -\frac{\omega_O \cdot r_2}{g \cdot b_2 \cdot \left(\pi \cdot D_2 - n \cdot \frac{t}{\sin(\beta_2)}\right) \cdot \tan(\beta_2)}$$

$$-196\ \frac{s}{m^2} = -\frac{\left(2500 \frac{rev}{\min} \cdot \frac{min}{60\text{s}} \cdot \frac{2\pi\ rad}{rpm}\right) \cdot (0.11842\ m)}{\left(9.81\ \frac{m}{s^2}\right) \cdot (0.0323362\ m) \cdot \left(\pi \cdot (0.236855\ m) - 10 \cdot \frac{(0.0047625\ m)}{\sin(\beta_2)}\right) \cdot \tan(\beta_2)}$$

$$-196\ \frac{s}{m^2} = -\frac{\left(31.0042\ \frac{m \cdot rad}{s}\right)}{0.31722\ \frac{m^2}{s^2} \cdot \left((0.7441\ m) - \frac{(0.047625\ m)}{\sin(\beta_2)}\right) \cdot \tan(\beta_2)}$$

$$-196\ \frac{s}{m^2} = -\frac{\left(31.0042\ \frac{m \cdot rad}{s}\right)}{\left((0.23604 \frac{m^3}{s^2}) - \frac{\left(0.01511\ \frac{m^3}{s^2}\right)}{\sin(\beta_2)}\right) \cdot \tan(\beta_2)}$$

$$\beta_2 = 0.64\ rad \cdot \frac{180°}{\pi \cdot rad} = 36.67°$$

Manometer Fluid Density: In the following equation ρ_f is the density of the manometer fluid, SG is the specific gravity of the manometer fluid, and ρ_r is the density of the reference material which in our case is water.

$$\rho_f = SG \cdot \rho_r$$

$$\rho_f = 0.827 \cdot 1000\ \frac{kg}{m^3}$$

$$\rho_f = 827\ \frac{kg}{m^3}$$

Air Density: In the following equation P_{atm} is the atmospheric pressure of air, T_{atm} is the atmospheric temperature of air, R_{air} is the ideal gas constant for air, R_{vapor} is the gas constant for water vapor, P_g is the saturation pressure at atmospheric temperature, ϕ_{atm} is the relative humidity of the air, and ρ_a is the density of air at room temperature.

$$\rho_a = \frac{P_{atm}}{R_{air} \cdot T_{atm}} + \frac{\phi_{atm}}{100\%} \cdot \frac{P_g}{T_{atm}} \cdot \left(\frac{1}{R_{vapor}} - \frac{1}{R_{air}}\right)$$

$$\rho_a = \frac{763.22\ mmHg \cdot 133.322 \frac{Pa}{mmHg}}{\left(286.9\ \frac{N \cdot m}{kg \cdot \cancel{K}}\right) \cdot 293.93\ \cancel{K}} + \frac{51\%}{100\%} \cdot \frac{2451.9 \frac{N}{m^2}}{293.93\ K} \cdot \left(\frac{1}{461.5 \frac{N\ m}{kg\ K}} - \frac{1}{286.9 \frac{N\ m}{kg\ K}}\right)$$

$$\rho_a = \frac{101751.6\ \cancel{Pa} \cdot \frac{1\ \frac{\cancel{N}}{m^2}}{1\ \cancel{Pa}}}{84328.5\ \frac{\cancel{N} \cdot m}{kg \cdot \cancel{K}}} + 0.51 \cdot 8.342\ \frac{\cancel{N}}{m^2\ \cancel{K}} \cdot -0.001319\ \frac{kg\ \cancel{K}}{\cancel{N}\ m}$$

$$\rho_a = 1.201\ \frac{kg}{m^3}$$

Inlet Nozzle Area: In the following equation A is the cross-sectional area of the inlet and D is the diameter of the inlet.

$$A = \frac{\pi \cdot D^2}{4}$$

$$A = \frac{\pi \cdot (0.075\ m)^2}{4}$$

$$A = 0.004418\ m^2$$

Inlet Velocity: In the following equation V is the velocity of the fluid, g is the gravitational constant, h_4 is the height of the manometer fluid open to the atmosphere, h_1 is the height of the manometer fluid connected to the inlet, ρ_f is the density of the manometer fluid, and ρ_a is the density of the air. The following calculation is of the impeller at 100% flowrate at an angular velocity of 2500 rpm.

$$V = \sqrt{\frac{2 \cdot \rho_f \cdot g \cdot (h_1 - h_4)}{\rho_a}}$$

$$V = \sqrt{\frac{2 \cdot 827\ \frac{\cancel{kg}}{\cancel{m^3}} \cdot 9.81\ \frac{m}{s^2} \cdot (18.0\ cm - 11.8\ cm)}{1.2015\ \frac{\cancel{kg}}{\cancel{m^3}}}}$$

$$V = \sqrt{83728.33\ \frac{\cancel{cm} \cdot m}{s^2} \cdot \frac{1m}{100\ \cancel{cm}}}$$

$$V = \sqrt{837.28\ \frac{m^2}{s^2}}$$

$$V = 28.9353\ \frac{m}{s}$$

Volumetric Flowrate: In the following equation V is the velocity of the fluid, A is the cross-sectional area of the inlet, and Q is the volumetric flowrate of the fluid. The following calculation is of the impeller at 100% flowrate at an angular velocity of 2500 rpm.

$$Q = V \cdot A$$

$$Q = \left(28.935\ \frac{m}{s}\right) \cdot (0.004418\ m^2)$$

$$Q = 0.1278 \frac{m^3}{s}$$

Mass Flowrate: In the following equation $\dot{m}$ is the mass flowrate of the fluid, ρ_a is the density of the air, and Q is the flowrate of the fluid. The following calculation is of the impeller at 100% flowrate at an angular velocity of 2500 rpm.

$$\dot{m} = Q \cdot \rho_a$$

$$\dot{m} = \left(0.1278 \frac{\cancel{m^3}}{s}\right) \cdot \left(1.2015 \frac{kg}{\cancel{m^3}}\right)$$

$$\dot{m} = 0.1535 \frac{kg}{s}$$

Head: In the following calculation H_a is the head available, h_3 is the height of the manometer fluid connected after the impeller, h_2 is the height of the manometer fluid connected before the impeller, g is the gravitational constant, ρ_f is the density of the manometer fluid, and ρ_a is the density of the air. The following calculation is of the impeller at 100% flowrate at an angular velocity of 2500 rpm.

$$H_a = \frac{\rho_f \cdot (h_2 - h_3)}{\rho_a}$$

$$h_a = \frac{827 \frac{\cancel{kg}}{\cancel{m^3}} \cdot (12.9\ cm - 11.5\ cm)}{1.2015 \frac{\cancel{kg}}{\cancel{m^3}}}$$

$$h_a = 963.628\ cm$$

$$h_a = 9.636\ m$$

Torque: In the following equations T is the torque of the impeller, g is the gravitational constant, d is the motor arm distance, y is the mass, F is the force, and v is the voltage. The following calculation is of the impeller at 100% flowrate at an angular velocity of 2500 rpm. In order to calculate the torque, known masses were placed on the lever arm and the resulting voltage was recorded. The mass was plotted vs. voltage and the line of best fit was calculated. The force is calculated from voltage reading by using this relationship between mass and voltage.

$$T = F \cdot d$$

$$y = \left(186.65255 \frac{g}{mV}\right) \cdot v - 182.8863\ g$$

$$y = \left(186.65255 \frac{g}{\cancel{mV}}\right) \cdot 2.29\ \cancel{mV} - 182.8863\ g$$

$$y = 244.548\ g$$

$$F = y \cdot g$$

$$F = 0.244548\ kg \cdot 9.81 \frac{m}{s^2}$$

$$F = 2.399\ N$$

$$T = 2.399\ N \cdot 0.179\ m$$

$$T = 0.4294\ N \cdot m$$

Brake Horsepower: In the following equation *BHP* is the break horsepower, *T* is the torque, and ω is the angular velocity. The following calculation is of the impeller at 100% flowrate at an angular velocity of 2500 rpm.

$$BHP = T \cdot \omega$$

$$BHP = (0.4294\ N \cdot m) \cdot \left(2500 \frac{\cancel{rev}}{\cancel{min}} \cdot \frac{\cancel{min}}{60 \cdot s} \cdot \frac{2\pi}{\cancel{rev}}\right)$$

$$BHP = 112.422\ W$$

Water Horsepower: In the following equation *WHP* is the water horsepower, *Q* is the volumetric flowrate of the fluid, H_a is the head available, and γ is the specific weight of air. The following calculation is of the impeller at 100% flowrate at an angular velocity of 2500 rpm.

$$WHP = Q \cdot \gamma \cdot H_a$$

$$WHP = \left(0.1278\ \frac{\cancel{m^3}}{s}\right) \cdot \left(11.77\ \frac{N}{\cancel{m^3}}\right) \cdot 9.636\ m$$

$$WHP = 14.498\ W$$

Pump Efficiency: In the following equation η is the overall pump efficiency, *WHP* is the water horsepower, and *BHP* is the break horsepower. The following calculation is of the impeller at 100% flowrate at an angular velocity of 2500 rpm.

$$\eta = \frac{WHP}{BHP}$$

$$\eta = \frac{14.498\ W}{112.422\ W}$$

$$\eta = 0.12896$$

$$\eta = 12.896\ \%$$

Air Density Uncertainty: In the following equations ρ_a is the density of the air, $U(\rho_a)$ is the uncertainty in the density of the air, P_{atm} is the atmospheric pressure, $U(P_a)$ is the uncertainty in the atmospheric pressure, R_{air} is the ideal gas constant for air, R_{vapor} is the ideal gas constant for the vapor, T_{atm} is the atmospheric temperature, $U(T_{atm})$ is the uncertainty in the atmospheric temperature, ϕ_{atm} is the relative humidity at atmospheric conditions, $U(\phi_{atm})$ is the uncertainty in the atmospheric relative humidity, and P_g is the pressure of the gas.

$$\rho_a = \frac{P_{atm}}{R_{air} \cdot T_{atm}} + \frac{\phi_{atm}}{100\%} \cdot \frac{P_g}{T_{atm}} \cdot \left(\frac{1}{R_{vapor}} - \frac{1}{R_{air}}\right)$$

$$U_{\rho_a} = \sqrt{\left(\frac{\partial \rho_a}{\partial P_{atm}} U_{P_{atm}}\right)^2 + \left(\frac{\partial \rho_a}{\partial T_{atm}} U_{T_{atm}}\right)^2 + \left(\frac{\partial \rho_a}{\partial \phi_{atm}} U_{\phi_{atm}}\right)^2}$$

$$\frac{\partial \rho_a}{\partial P_{atm}} = \frac{1}{R_{air}\ T_{atm}}$$

$$\frac{\partial \rho_a}{\partial T_{atm}} = -\frac{P_{atm}}{R_{air} \cdot T_{atm}^2} - \frac{\phi_{atm}}{100\%} \cdot \frac{P_g}{T_{atm}^2} \cdot \left(\frac{1}{R_{vapor}} - \frac{1}{R_{air}}\right)$$

$$\frac{\partial \rho_a}{\partial \phi_{atm}} = \frac{1}{100\%} \cdot \frac{P_g}{T_{atm}} \cdot \left(\frac{1}{R_{vapor}} - \frac{1}{R_{air}} \right)$$

$$\frac{\partial \rho_a}{\partial P_{atm}} = \frac{1}{\left(286.9 \frac{N \cdot m}{kg \cdot \cancel{K}} \right) \cdot 293.93 \, \cancel{K}}$$

$$\frac{\partial \rho_a}{\partial P_{atm}} = 1.186 \times 10^{-5} \frac{kg}{N \, m}$$

$$U_{\rho_a} = \sqrt{\begin{array}{l} \left(1.186 \times 10^{-5} \frac{kg}{\cancel{N} \, m} \cdot 763.22 \, mmHg \cdot 133.322 \frac{Pa}{mmHg} \cdot \frac{1 \frac{\cancel{N}}{m^2}}{1 \, \cancel{Pa}} \right)^2 \\ + \left(-4.086 \times 10^{-3} \frac{kg}{m^3 \, \cancel{K}} \cdot 0.0556 \, \cancel{K} \right)^2 + \left(-1.1 \times 10^{-4} \frac{kg}{m^3} \cdot 0.5 \right)^2 \end{array}}$$

$$U_{\rho_a} = 2.47 \times 10^{-4} \frac{kg}{m^3}$$

Volumetric Flowrate Uncertainty: In the following equation Q is the volumetric flowrate of the fluid (air), $U(Q)$ is the uncertainty in the volumetric flowrate, D_n is the diameter of the nozzle, ρ_f is the density of the manometer fluid, h_1 is the height of the fluid in the first manometer, h_4 is the height of the fluid in the 4th manometer, and ρ_a is the density of air.

$$Q = \frac{\pi D_n^2}{4} \cdot \sqrt{\frac{2 \cdot \rho_f \cdot g \cdot (h_1 - h_4)}{\rho_a}}$$

$$U_Q = \sqrt{\begin{array}{l} \left(3.410 \frac{m^2}{s} \cdot 0.0005 \, m \right)^2 + \left(-1.031 \frac{m^2}{s} \cdot 0.001 \, m \right)^2 \\ + \left(1.031 \frac{m^2}{s} \cdot 0.001 \, m \right)^2 + \left(-0.0532 \frac{m^6}{\cancel{kg} \, s} \cdot 2.47 \times 10^{-4} \frac{\cancel{kg}}{m^3} \right)^2 \end{array}}$$

$$U_Q = 2.243 \times 10^{-3} \frac{m^3}{s}$$

Head Uncertainty: In the following equations H_a is the head available, $U(H_a)$ is the uncertainty in the head available, ρ_f is the density of the manometer fluid, ρ_a is the density of air, h_2 is the height of the fluid in the 2nd manometer, and h_3 is the height of the fluid in the 3rd manometer.

$$H_a = \frac{\rho_f \cdot (h_2 - h_3)}{\rho_a}$$

$$U_{H_a} = \sqrt{\left(\frac{\partial H_a}{\partial \rho_a} U_{rho_a} \right)^2 + \left(\frac{\partial H_a}{\partial h_2} U_{h_2} \right)^2 + \left(\frac{\partial H_a}{\partial h_3} U_{h_3} \right)^2}$$

$$U_{H_a} = \sqrt{\left(-8.027 \frac{m^4}{\cancel{kg}} \cdot 2.47 \times 10^{-4} \frac{\cancel{kg}}{\cancel{m^3}} \right)^2 + (6.886 \cdot 0.001 \, m)^2 + (-6.886 \cdot 0.001 \, m)^2}$$

$$U_{H_a} = 0.973 \, m$$

PumpLinx® Adjustment Methodology

Our group decided to first adjust the β_1 and β_2 values and determine if modification of these angles would result in a closer match of our simulated curve to the given curve. Each angle was adjusted positively and negatively individually, resulting in four graphs. First, decreasing β_2 brought the curve closer to the desired curve than increasing β_2. Adjusting β_2 from 36.865^o to $32°$ resulted in the simulated curve being closer to the given curve, but sloped down too much.

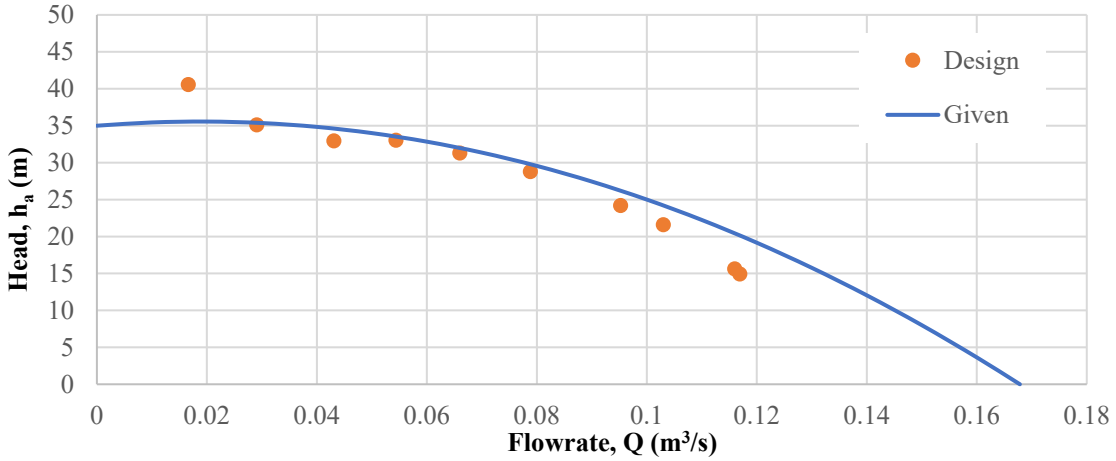

Figure 5: The second iteration of the impeller's head is plotted vs flowrate. The impeller's β_2 angle was decreased and this resulted in more negative slope of its performance curve. The error resulting from this plot is 9.51%, which is outside the desired percent of error.

In figure 6 below, β_1 was adjusted from 15.012^o to be 20^o while $\beta_2 = 36.865^o$ and resulted in slope that did not match up much better to the given curve. The decision to keep $\beta_1 = 15.012^o$ was made and adjustments of other parameters will be performed moving forward.

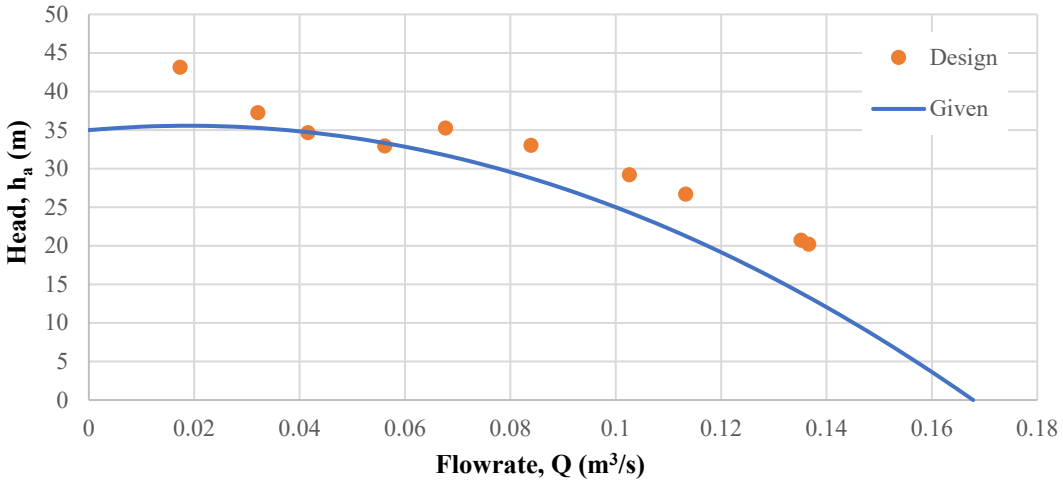

Figure 6: The 3rd iteration of our impeller design's head was plotted vs. flowrate. This design iteration altered only the β_1 angle by increasing it and it resulted in an increasingly negative slope compared to the second iteration and a minimal reduction in the shutoff head. The error resulting from this plot is 20.09% which is outside the desired percent of error.

After we settled on blade angles of $\beta_1 = 15.01°$ and $\beta_2 = 35°$, the shape of the blade was adjusted and tested to determine how the performance of the impeller was affected in the simulation. Rather than using an arc of constant radius from end to end, we adjusted the shape to have a more drastic curve (or smaller radius) near the entrance end and be linear toward the exit end of the blade. We referred to this design as the "Low Curve" due to the location of the curved portion of the blade. The resulting simulation curve resulted in a more desirable slope when the flowrate was above 0.06. The curve slope before a flowrate of 0.04 was too steep and didn't match the given curve very well.

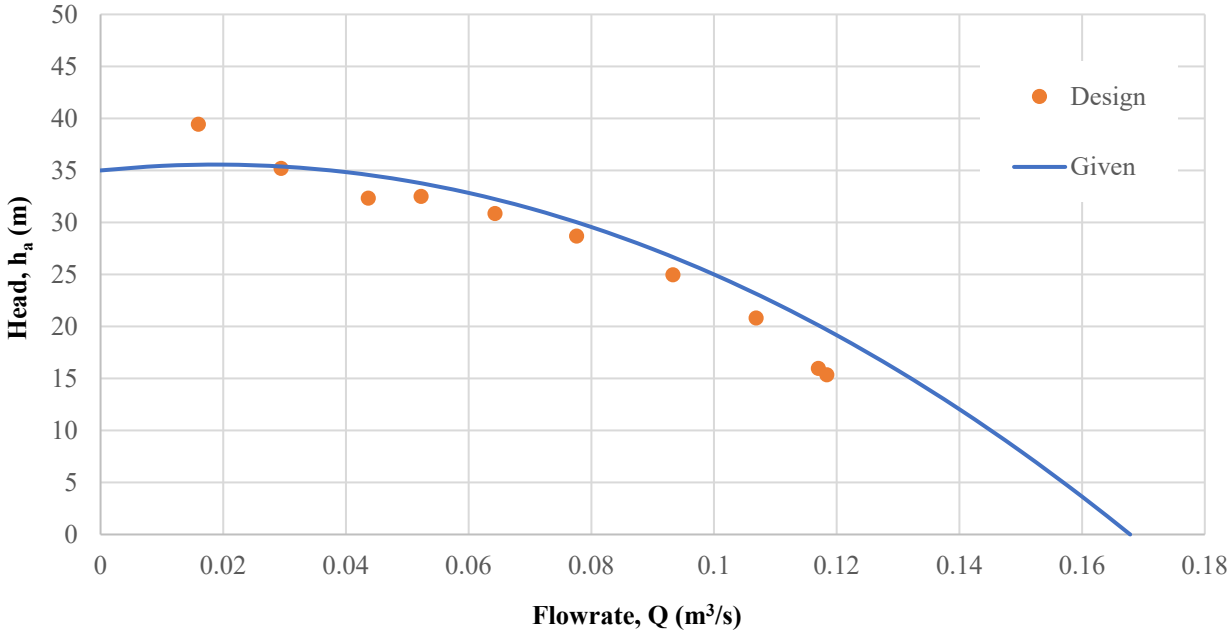

Figure 7: The 4th iteration of our impeller design's head was plotted vs. flowrate. This iteration the impeller's blade shape was altered, and this resulted in minimal changes to the slope and the shutoff head from the previous iterations curve. This iteration was the alteration of the blade shape by decreasing the arc of the blade from the beginning of the blade to the midpoint. The error resulting from this plot is 8.99% which is outside the desired percent of error.

The shape of the blade was adjusted for a second iteration to determine how the performance of the impeller was affected in the simulation. This time we placed the curved portion of the blade near the exit while making the entrance end of the blade linear, which we refer to as "High Curve". The resulting simulation curve resulted in a more desirable slope when the flowrate was under 0.06. The curve slope after a flowrate of 0.06 was too steep and didn't match the given curve very well. It was also noted that the overall head of this simulated curve was higher in the portion after the flowrate reached 0.06.

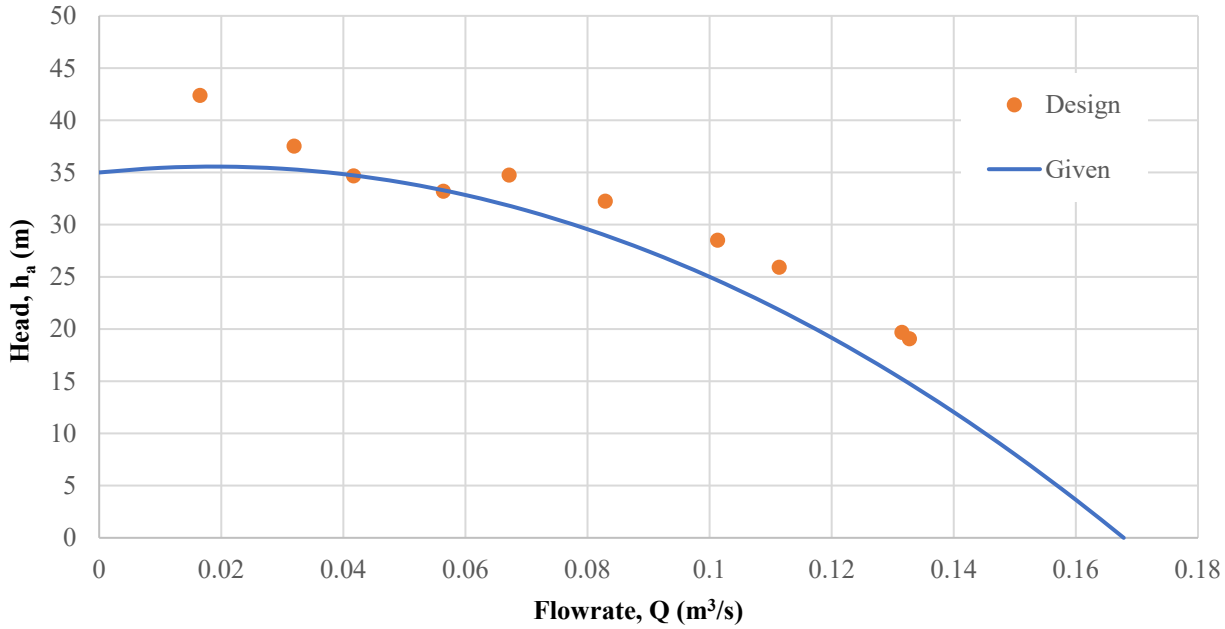

Figure 8: The 5th iteration of the impeller design's head was plotted vs. flowrate. The behavior of the designed impeller's performance curve is that it has an much higher shutoff head than the previous iteration and its slope is also greater than the previous iteration. This iteration was the alteration of the blade shape by increasing the arc of the blade from the midpoint of the blade. The error resulting from this plot is 13.93% which is outside the desired percent of error.

Our group decided to attempt to mix different aspects of the Low Curve and High Curve to produce an impeller that can minimizes the error between the simulated curve and the given curve. The final iteration of the impeller design is a "Middle Curve" design that showcases straight portions at the entrance and exit ends of the blade, with the curve in the middle. This was selected to combine the desirable aspects of both the low curve and high curve blade designs observed previously. The β_1 and β_2 were left at 15.01° and 35°, respectively. Combining all this knowledge resulted in the following simulated performance curve, documented later in the report. The given and simulated curves match up very well and showcase an error of 4% when considering all points. When the first point in the simulated curve is not considered since it only occurs at very low flowrates, the error goes down to 2%. This design is within the desired error of 5%.

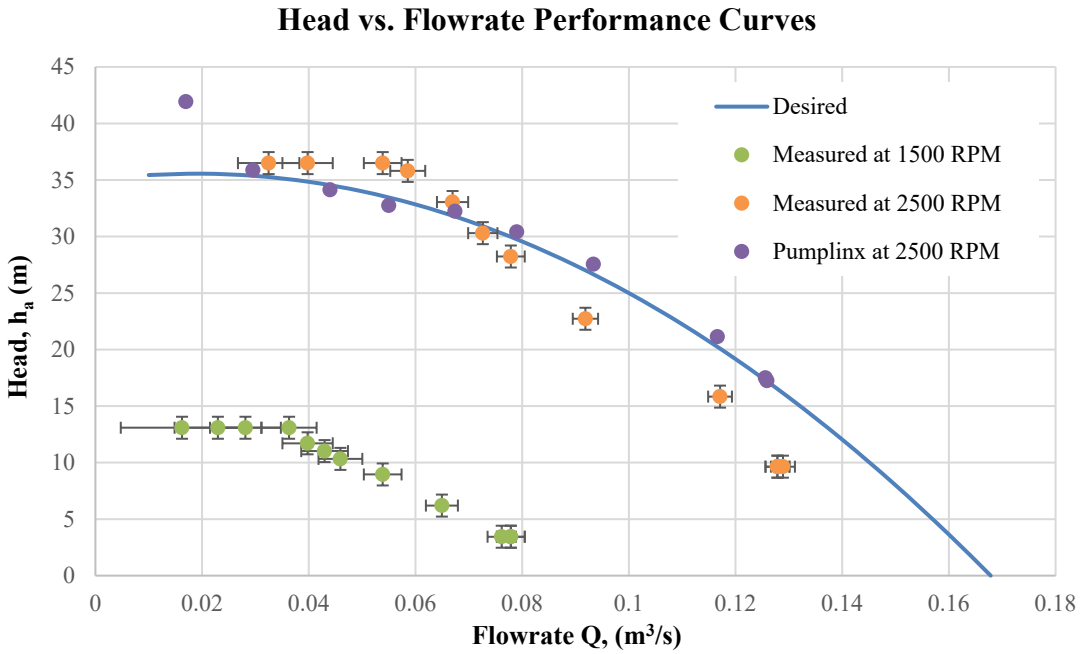

Figure 9: The desired performance curve plotted along with the theoretical performance curve generated through PumpLinx®, the measured performance curve generated by testing the physical impeller at 1500 RPM, and the measured performance curve generated by testing the physical impeller at 2500 RPM. The uncertainties in the measurements and calculations for the physical tests are also included.

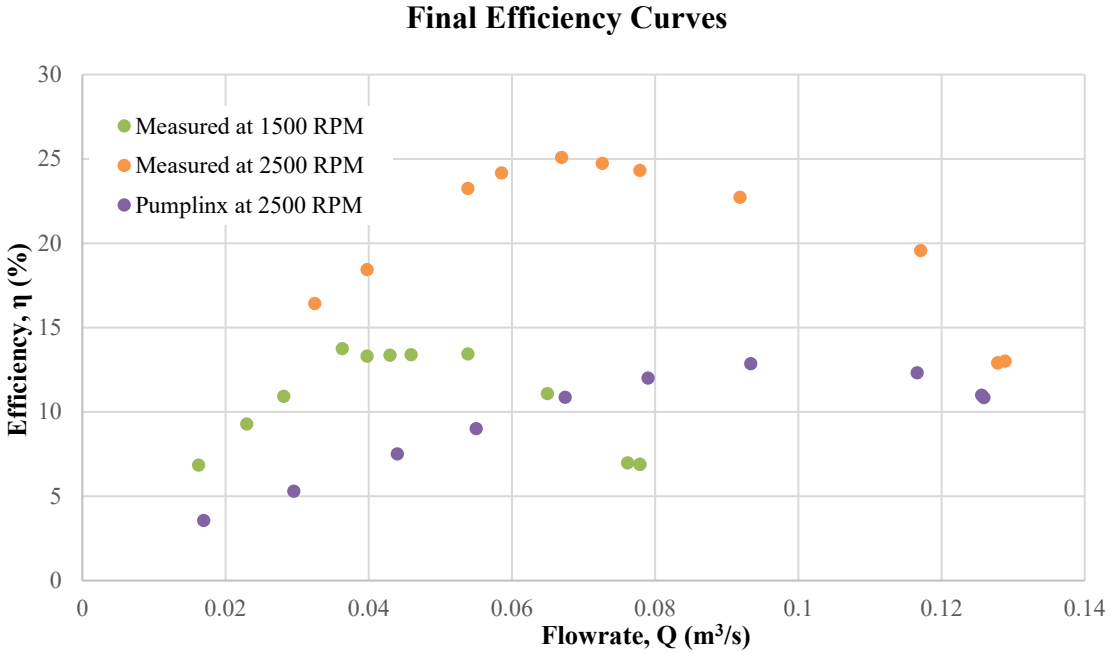

Figure 10: The efficiency curves generated by the PumpLinx® simulation at 2500 RPM, the physical model tested at 1500 RPM, and the physical model tested at 2500 RPM.

ROTATION: COUNTER-CLOCKWISE

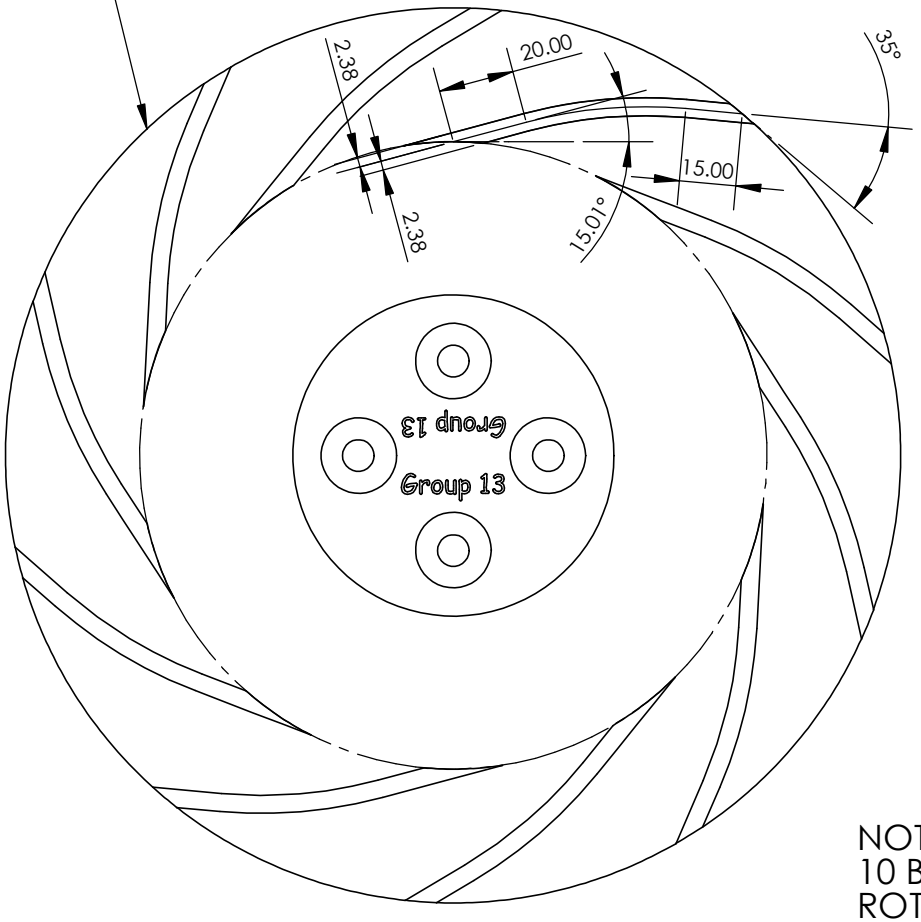

NOTE:
10 BLADES
ROTATION COUNTER-CLOCKWISE

EML4147C: THERMODYNAMICS LAB	**TEAM: Group 13**	**PART NAME: Group13_Final_Impeller**
UF Herbert Wertheim College of Engineering, Department of Mechanical & Aerospace Engineering, UNIVERSITY of FLORIDA	**DESIGN ENGINEER: CYRIL M., HUNTER E., NICKOLAS S.**	
	MATERIAL:	**PART NUMBER: EML4147C_1**

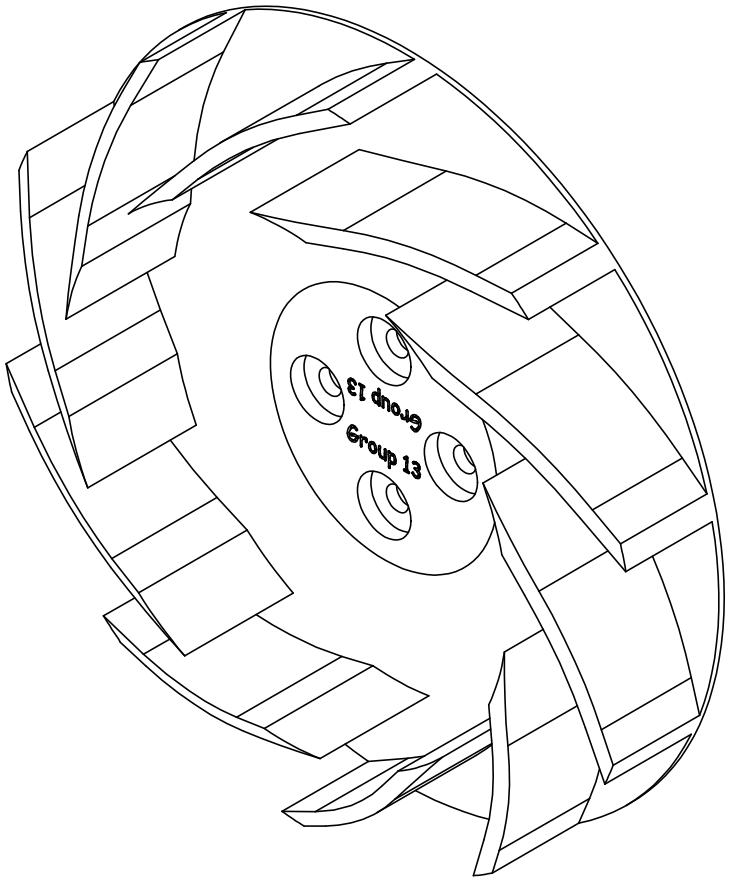

EML4147C: THERMODYNAMICS LAB UF Herbert Wertheim College of Engineering *Department of Mechanical & Aerospace Engineering* UNIVERSITY *of* FLORIDA	TEAM: Group 13	PART NAME: Group13_Final_Impeller
	DESIGN ENGINEER: CYRIL M., HUNTER E., NICKOLAS S.	
	MATERIAL:	PART NUMBER: EML4147C_1

Final Design Summary and Recommendations

The objective of this report was to design an impeller to produce a specified performance curve and to compare and analyze the impeller CFD analysis results, the physical impeller testing results, and the given theoretical performance curves.

For the CFD performance curve, results showcased an error between 2% and 4% when compared to the given theoretical curve. The physical testing performance curve resulted in an error of 16.5% when compared to the given theoretical curve. This can be due to several discrepancies such as leaking air due to the testing apparatus, layer lines due to 3-D printing, and inaccuracies in measurements.

The accuracy of the testing apparatus is important to consider and a recommendation to lower the error resulting from impeller testing would be to ensure no air leaks in the testing apparatus. Another aspect to consider is the nature of 3-D printing resulting in rough edges along the blades and impeller affecting the impeller performance. To mitigate this issue, it is recommended that slight sanding down of the blades and edges to help reduce the error. Another recommendation would be to use another manufacturing method for the impeller that doesn't result in layer lines and rough edges or blades. Another recommendation is to account for the additional 12.5% to 14.5% impeller testing error when creating the impeller design.

EML 4304C			Design Project Log		
Date	Name	Time in	Time out	Total time	Description of tasks
4/4/2022	Cyril Moran	1:00	3:00	2	Planned out what needed to be done for the FDR, Set-up impeller test meeting
4/4/2022	Nickolas Saavedra	1:00	3:00	2	Planned out what needed to be done for the FDR, Set-up impeller test meeting
4/4/2022	Hunter Enos	1:00	3:00	2	Planned out what needed to be done for the FDR, Set-up impeller test meeting
4/7/2022	Cyril Moran	1:00	2:00	1	Impeller testing session
4/7/2022	Nickolas Saavedra	1:00	2:00	1	Impeller testing session
4/7/2022	Hunter Enos	1:00	2:00	1	Impeller testing session
4/8/2022	Hunter Enos	4:00	6:00	2	Head, velocity, torque calculations
4/14/2022	Cyril Moran	1:00	3:30	2.5	Fixed the head, torque, BHP and WHP calculations
4/14/2022	Nickolas Saavedra	11:30	3:00	3.5	Fixed the head, torque, BHP and WHP calculations. Began correcting report abstract and introduction
4/14/2022	Hunter Enos	11:30	2:00	2.5	Made graphs, added to intro
4/14/2022	Cyril Moran	4:30	6:30	2	Added all of the sample calculations
4/17/2022	Nickolas Saavedra	5:30	7:00	1.5	Corrected introduction, began recommendations.
4/18/2022	Nickolas Saavedra	9:30	11:30	2	Corrected calculations for 3-D printed impeller performance graph
4/18/2022	Hunter Enos	12:00	3:00	3	Uncertianty Calcs
4/20/2022	Cyril Moran	12:30	2:30	2	Fixed the blade angle derivations, and finished the introduction.
4/20/2022	Nickolas Saavedra	10:00	12:30	2.5	Corrected introduction, proofread report, derived equations for blade angle equations
4/20/2022	Cyril Moran	4:30	7:30	3	Updated the disucssion section and helped with formatting
4/20/2022	Nickolas Saavedra	4:30	7:30	3	Continued deriving equations for blade angle, Wrote recommendations and summary, completed report
4/20/2022	Hunter Enos	10:00	2:00	4	Intro diagrams, finished modeling section
4/20/2022	Hunter Enos	4:30	7:30	3	Intro diagrams, graph formatting
			Total:	45.5	